

# Influence of Subphase Conditions on Interfacial Viscoelastic Properties of Synthetic Lipids with Gentiobiose Head Groups

Motomu Tanaka,<sup>\*,†</sup> Stefan Schiefer,<sup>†</sup> Christian Gege,<sup>‡</sup> Richard R. Schmidt,<sup>‡</sup> and Gerald G. Fuller<sup>§</sup>

*Lehrstuhl für Biophysik E22, Technische Universität München, D-85748 Garching, Germany, Fachbereich Chemie, Universität Konstanz, Fach M 725, D-78457 Konstanz, Germany, and Department of Chemical Engineering, Stanford University, Stanford, California 94305-5025*

*Received: September 18, 2003; In Final Form: December 10, 2003*

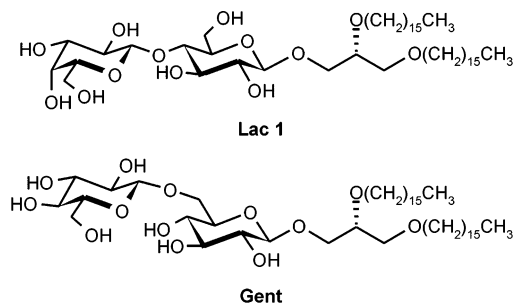
The thermodynamic parameters and rheological properties of a synthetic glycolipid with a gentiobiose (*O*-( $\beta$ -D-glucopyranosyl)-(1 $\rightarrow$ 6- $\beta$ -D-glucopyranoside)) headgroup have been studied at the air/water interface. The phase transition entropy and latent heat were estimated by film balance experiments at various temperatures, whereas dynamic surface moduli (loss and storage modulus) were measured by an interfacial stress rheometer under well-defined thermodynamic conditions. The impact of glucosidic bonding was systematically studied by comparing the measured results to those from the lipid with a lactose (*O*-( $\beta$ -D-galactopyranosyl)-(1 $\rightarrow$ 4- $\beta$ -D-glucopyranoside)) headgroup, which possesses the similar monosaccharide composition. We found that the “bent” 1 $\rightarrow$ 6 junction of gentiobiose reduces the lateral intermolecular cooperativity and fluidizes the films in comparison to the lactose lipid monolayer.

## Introduction

Surfaces of plasma membranes are rendered with glycocalices, which are oligo- and polysaccharide chains adjacent to glycolipids, peptidoglycans, and glycoproteins. They serve as stabilizers to retain plasma membrane structures as well as “repellers” to maintain a certain distance between neighboring cells.<sup>1</sup> They assume a stable conformation via relatively weak (generic) forces, like electrostatic interactions, hydrogen bonding, and long-range van der Waals interactions, which can be established with the specific counterparts (e.g., receptors, complimentary carbohydrates).<sup>1,2</sup> One of the experimental approaches to study the complex interplay of various forces on plasma membrane surfaces is the measurement of the mechanical properties of a glycocalix.<sup>3,4</sup> As simplified glycocalix models, we chose monolayers of synthetic glycolipids with cylindrical headgroups, and studied the interfacial viscoelastic properties using an interfacial stress rheometer (ISR).<sup>5,6</sup> This device enables the effects of the hydrophobic/hydrophilic balance on interfacial rheology to be studied quantitatively. The observed rheological transitions indeed reflected changes in in-plane cooperativity in the films that accompany a thermodynamic phase transition.<sup>7</sup> Moreover, structural investigations at short length scales further demonstrated that a viscous-to-elastic transition monitored by the ISR coincides with physical cross-linking between the carbohydrate headgroups via dehydration of the headgroups.<sup>8,9</sup>

A neo-glycolipid was synthesized with a gentiobiose (*O*-( $\beta$ -D-glucopyranosyl)-(1 $\rightarrow$ 6- $\beta$ -D-glucopyranoside)) headgroup (Gent, Chart 1 bottom). As recently reported, gentiobiose is claimed to be responsible for the toxicity of lipoteichoic acid (LTA) in gram positive bacteria, which is similar to the role of lipid A in

**CHART 1: Chemical Structures of Neo-glycolipids with Gentiobiose (*O*-( $\beta$ -D-glucopyranosyl)-(1 $\rightarrow$ 6- $\beta$ -D-glucopyranoside)) Head Group (Gent lipid, bottom) and Lactose (*O*-( $\beta$ -D-galactopyranosyl)-(1 $\rightarrow$ 4- $\beta$ -D-glucopyranoside)) Head Group (Lac 1 lipid, top)**



gram negative bacteria.<sup>1</sup> In the first part of this study, we studied the thermodynamic phase behavior of the Gent monolayer at various temperatures and estimated thermodynamic parameters quantitatively. In the second part, the strength of hydrogen bonding was enhanced by changing the subphase from deionized water to D<sub>2</sub>O, and the influence on the in-plane cooperativity was studied using the ISR. The experimental results are also systematically compared to those from the lipid with a monolactose (*O*-( $\beta$ -D-galactopyranosyl)-(1 $\rightarrow$ 4)- $\beta$ -D-glucopyranoside)) headgroup (Lac 1, Chart 1 top). This glycolipid possesses an identical lipid anchor and glycerol junction, which are linked to a similar monosaccharide component as Gent lipid. We observed a clear impact of headgroup conformation (steric effects) on the viscoelastic properties.

## Materials and Methods

Synthesis of Gent lipid was achieved using the reaction route presented in Scheme 1. Activation of known gentiobiose heptaacetate **1**<sup>10</sup> with trichloroacetonitrile in the presence of

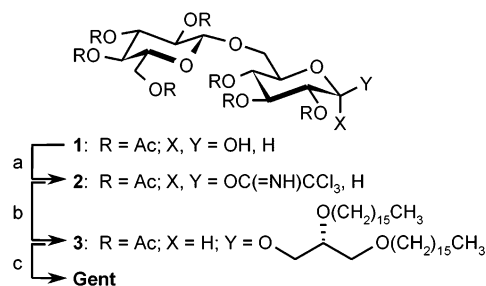
\* To whom correspondence should be addressed. Fax: +49-8928912469. E-mail: mtanaka@ph.tum.de.

<sup>†</sup> Technische Universität München.

<sup>‡</sup> Universität Konstanz.

<sup>§</sup> Stanford University.

## SCHEME 1: Synthesis of Gent Glycolipid



(a) CCl<sub>3</sub>CN, DBU, 72%; (b) 1,2-di-*O*-hexadecyl-*sn*-glycerol, 0.4 eq. TMSOTf, CH<sub>2</sub>Cl<sub>2</sub>, molecular sieves AW-300, rt, 45 min, 45%; (c) NaOMe, MeOH/CH<sub>2</sub>Cl<sub>2</sub>, 77%. DBU = 1,8-diazabicyclo[5.4.0]undec-7-ene, TMSOTf = trimethylsilyl trifluoromethanesulfonate.

DBU afforded trichloroacetimidate **2** in 72% yield (Scheme 1). Glycosidation of donor **2** with one equivalent of 1,2-di-*O*-hexadecyl-*sn*-glycerol<sup>11,12</sup> as a lipid anchor was performed in the presence of TMSOTf as a catalyst to give the gentiobiose intermediate **3** in 45% yield. The  $\beta$ -configuration of the newly formed glycosidic bond was confirmed in the <sup>1</sup>H NMR spectrum ( $J_{1,2}$  = 7.9 Hz). Finally, de-*O*-acetylation furnished the target Gent molecule. Synthesis of Lac 1 lipid has already been reported elsewhere.<sup>7</sup>

The spreading solutions for the monolayer deposition were prepared by dissolving each glycolipid into a mixture of chloroform/methanol (70/30 by volume) at a concentration of  $1 \times 10^{-3}$  M. To study the influence of the subphase on lateral hydrogen bonding among carbohydrate headgroups, we used two types of subphases: (1) deionized water ( $R > 18$  M $\Omega$ cm, Millipore, Molsheim, France) and (2) D<sub>2</sub>O (Sigma-Aldrich, Neu-Ulm, Germany). The viscoelastic parameters were measured by a self-built ISR, coupled to a Langmuir film balance (KSV Instruments, Helsinki, Finland).<sup>5</sup> A magnetized rod (length  $L$  = 50 mm, diameter  $\phi$  = 400  $\mu$ m) resides at the air/water interface and is confined in a narrow channel (channel width  $W$  = 6.4 mm). A sinusoidal magnetic field gradient was applied to translate the rod at a certain frequency  $\omega$ , and the displacement of the rod was monitored by a photodiode array. The translation of the rod causes a simple shear flow to occur at the interface.

The dynamic surface modulus,  $G^*(\omega) = G'(\omega) + iG''(\omega)$ , is a complex function where the real part (the elastic modulus,  $G'$  [mN/m]) is a measure of the elastic properties, and the imaginary part (the viscous modulus,  $G''$  [mN/m]) represents the viscous properties.<sup>13</sup> These two components can be related to each other by<sup>5</sup>

$$G'(\omega) + iG''(\omega) = \frac{\sigma_0}{\gamma_0} \exp(i\delta(\omega)) \quad (1)$$

and

$$\frac{G''(\omega)}{G'(\omega)} = \tan \delta(\omega) \quad (2)$$

$\sigma_0$  and  $\gamma_0$  correspond to the amplitudes of the interfacial drag (stress) and the displacement of the rod (strain), whereas  $\delta$  is the phase shift between the stress and strain.  $\sigma_0$  is equal to the amplitude of the applied force divided by  $2L$  because of the symmetry of the drag along the rod:  $\sigma_0 = F_0/2L$ .  $\gamma_0$  is the amplitude of the displacement normalized by the distance between the rod and the glass wall:  $\gamma_0 = 2x_0/W$ . The phase shift  $\delta$  is 0° when the film is purely elastic, whereas  $\delta$  of a

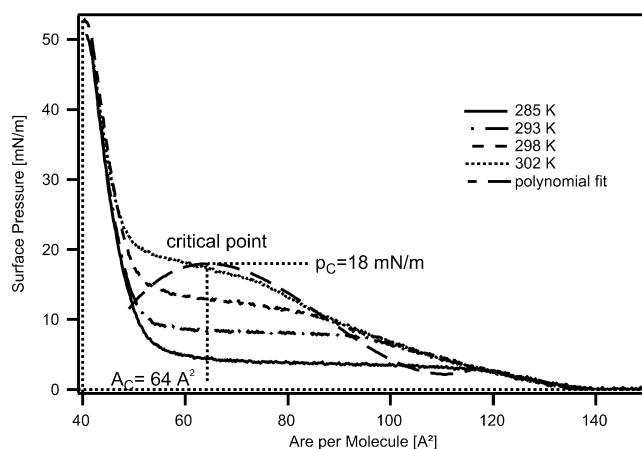


**Figure 1.** Pressure–area isotherms of Gent monolayers on H<sub>2</sub>O subphase at various temperature conditions. Phase coexistence regime was fitted by polynomial of fourth order, yielding critical surface area and pressure.

purely viscous film is 90°. Thus, this device allows quantitative measurements of both the elastic modulus  $G'$  and the viscous modulus  $G''$  under well defined thermodynamic conditions. The rheology experiments were carried out at 293 K, and the frequency of the oscillation was set constant at  $\omega = 0.92$  rad/s, if not stated otherwise.

## Results and Discussion

**Thermodynamic Phase Behaviors.** Figure 1 shows the surface pressure–area isotherms of Gent monolayers measured at  $T = 285, 293, 298$ , and  $302$  K. At all of the measurement conditions, we observed a plateaulike regime, which corresponds to the coexistence of liquid expanded and liquid condensed phases. The increase in temperature leads to a decrease in the coexistence region and an increase in the transition pressure. Such a systematic tendency coincides with the approach to a critical (or tricritical) point, which was reported for various insoluble surfactant monolayers.<sup>14,15</sup> Furthermore, the slope of the coexistence region increased according to the subphase temperature, which implies a decrease in finite cooperativity in phase transition. This is in contrast to the ideal first-order phase transition, where one assumes infinite cooperativity. Such a tendency can be attributed to the increase in steric (i.e., entropic) repulsion between gentiobiose headgroups that reduces cooperative interaction between alkyl chains.<sup>16</sup>

Thermodynamic parameters, such as molar latent heat  $\Delta q$  and phase transition entropy  $\Delta s$ , can be estimated from variation of the transition pressure  $p_k$  [mN/m] with temperature  $T$  (Figure 2a) by applying Clausius–Clapeyron equation for two-dimensional systems:<sup>14</sup>

$$\frac{dp_k}{dT} = \frac{\Delta s}{(A_{LE} - A_{LC})} = \frac{\Delta q}{(A_{LE} - A_{LC})} \quad (3)$$

where  $A_{LE}$  and  $A_{LC}$  stand for the areas per molecule at onset and offset of the phase coexistence. At a high temperature, namely, in the vicinity of the critical point, the phase coexistence in the isotherm can be approximated well as a parabola, whose maximum coincides with a critical point. Expansion of the van der Waals equation near the critical point actually leads to

$$\frac{A - A_C}{A_C} = 2 \left( \frac{T_C - T}{T_C} \right)^2 \quad (4)$$

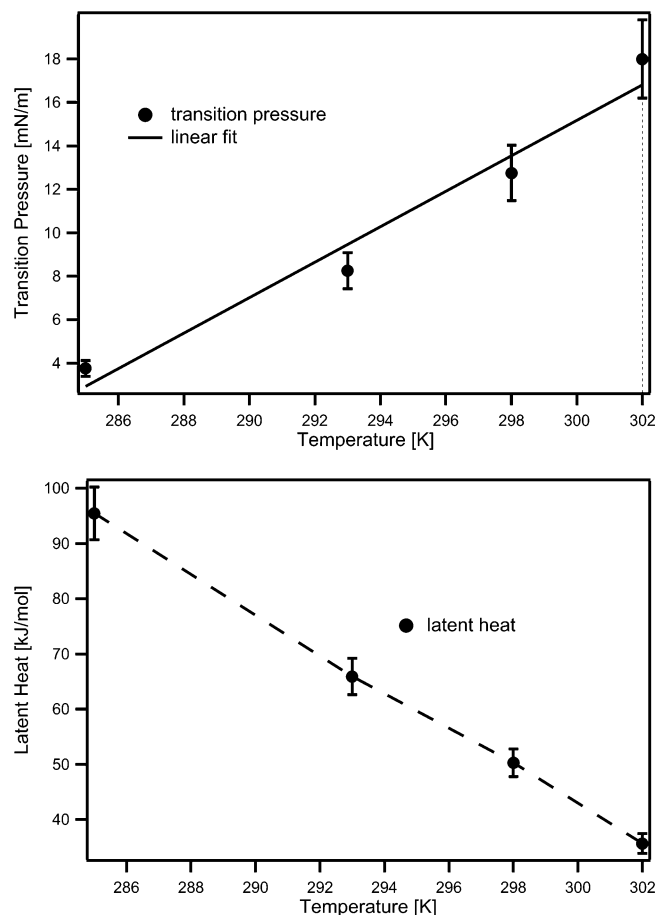


**Figure 2.** (a) Phase transition pressure ( $p_k$ ) and (b) molar latent heat ( $\Delta q$ ) of Gent monolayers plotted versus temperature  $T$ .

**TABLE 1: Thermodynamic Parameters of Gent and Lac 1 Monolayers<sup>a</sup>**

	$A_c^{\text{poly}}$ [ $\text{\AA}^2$ ]	$\Pi_c^{\text{poly}}$ [mN/m]	$\Pi_c^{\text{vdW}}$ [mN/m]	$T_c^{\text{vdW}}$
Gent	65	18	21	306
Lac 1	60	10	13	316

<sup>a</sup> The superscripts “poly” and “vdW” correspond to the values obtained by the polynomial fit and van der Waals gas model, respectively.

$A_C$  corresponds to the area at the maximum of the parabola. Here, both  $A_C$  and  $p_C$  can be derived by fitting the coexistence regime in Figure 1 with a polynomial of the fourth order,  $A_C = 64 \text{ \AA}^2$  and  $p_C = 18 \text{ mN/m}$ , respectively. Since  $\Delta q$  becomes zero at the critical point,  $T_C = 306 \text{ K}$  can be calculated from the extrapolation of  $\Delta q$  versus  $T$ :  $\Delta q(T_C) = 0$  (Figure 2b). By assuming a linear relationship between  $p_k$  and  $T$  (Figure 2a), one can thus obtain  $p_C = 21 \text{ mN/m}$ , which agrees well with that obtained from the parabola fit (Figure 1). The obtained numbers are summarized in Table 1, verifying the validity of our theoretical treatments.

#### Impact of Subphase Conditions on Viscoelastic Properties.

To compare the viscoelastic properties of different films, it is necessary to ensure that the rheological response from the system is independent from the degree of deformation. On the other hand, it is desirable to measure the rod's displacement at maximum amplitude. Thus, we first measured the dynamic modulus at various strain amplitudes and determined the optimal (maximum) strain amplitude for Gent monolayers,  $100 \text{ }\mu\text{m}$ . Figure 3 represents the elastic ( $G'$ ) and viscous ( $G''$ ) modulus of a Gent monolayer on  $\text{H}_2\text{O}$  water, plotted as a function of area per molecule. The isotherm at the same temperature ( $T =$

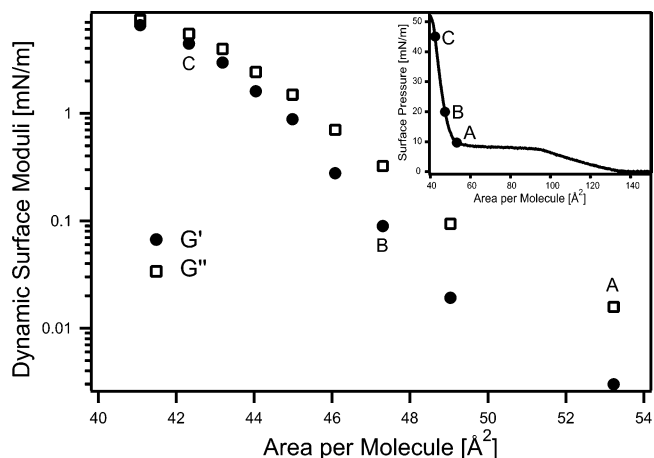


**Figure 3.** Viscoelastic properties of a Gent monolayer on  $\text{H}_2\text{O}$ . Storage ( $G'$ ) and loss ( $G''$ ) modulus are plotted as a function of area per molecule. Strain amplitude:  $100 \text{ }\mu\text{m}$ , frequency:  $0.92 \text{ rad/s}$ .

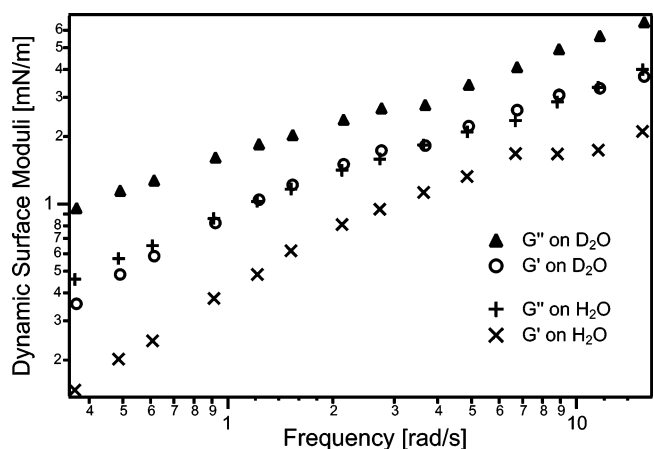


**Figure 4.** Dynamic modulus of Gent monolayers on  $\text{H}_2\text{O}$  and on  $\text{D}_2\text{O}$  measured at various frequencies. The surface pressure and the strain amplitude were kept constant,  $\pi = 25 \text{ mN/m}$  and  $100 \text{ }\mu\text{m}$ , respectively. Both  $G''$  and  $G'$  on  $\text{D}_2\text{O}$  subphase are always larger than the corresponding values on  $\text{H}_2\text{O}$  subphase.

$293 \text{ K}$ ) is given as an inset, where the correspondence between the isotherm and the dynamic modulus is indicated. The measured  $G''$  was larger than  $G'$  over a wide range of surface pressures, indicating that the film is predominantly viscous. Compression (i.e., lateral condensation) of the Gent monolayer led to a continuous increase both in  $G'$  and  $G''$ , resulting in a viscoelastic film ( $\tan \delta \sim 1$ ). In fact, increase in the dynamic modulus due to the film compression could also be observed for other insoluble surfactant monolayers.<sup>5,17</sup>

As the next step, influences of the subphase on lateral cooperativity in Gent monolayers were studied at  $25 \text{ mN/m}$  by measuring dynamic moduli on Purified water and on  $\text{D}_2\text{O}$  at various frequencies (Figure 4). On both subphases, Gent monolayers are predominantly viscous ( $G'' > G'$ ) over the whole frequency regime. However, it is notable that both  $G''$  and  $G'$  on  $\text{D}_2\text{O}$  subphase are always larger than the corresponding values on the water subphase. For example, at  $1 \text{ rad/s}$ , the dynamic moduli on the  $\text{D}_2\text{O}$  subphase are approximately two times larger than those on purified water. This finding can directly be attributed to the difference in the strength of hydrogen bonding mediated by  $\text{H}_2\text{O}$  and  $\text{D}_2\text{O}$ . As  $\text{D}\cdots\text{O}$  bonds are slightly stronger than  $\text{H}\cdots\text{O}$  bonds,  $\text{D}_2\text{O}$  causes stronger hydrogen bonding characteristics.<sup>18,19</sup> In spite of a clear deviation in viscoelastic parameters, we observed no differences in the pressure–area isotherms on these two subphases. The isotherm

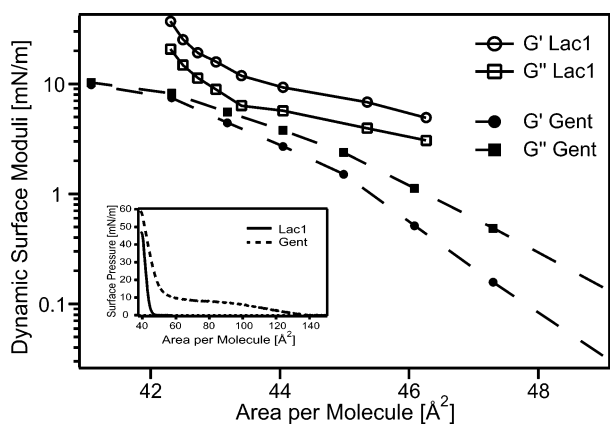


**Figure 5.** Dynamic modulus of Lac 1 and Gent monolayers plotted versus area per molecule. The corresponding pressure–area isotherms are given as insets.  $G''$  and  $G'$  of Lac 1 monolayers are always higher than those of Gent monolayers, implying steric effects of “bent” Gent headgroups.

on D<sub>2</sub>O totally overlaps with that on H<sub>2</sub>O and suggested no changes in lateral compressibility. The results obtained here thus demonstrated that ISR is very sensitive to the interfacial shear viscoelasticity of glycolipid monolayers, which cannot be detected by conventional film balance techniques.

Several previous studies postulated that hydrogen bonds between the ether oxygen of poly(ethylene oxide) and surrounding water molecules can be reduced by lowering the pH.<sup>20</sup> Naumann et al. reported that the rheological transition pressure of a lipopolymer monolayer at pH = 2.0 was smaller than that at pH = 5.5.<sup>21</sup> Here we titrated the pH of H<sub>2</sub>O from pH = 5.5 to pH = 2.0 with HCl and measured the dynamic modulus. Although it was difficult to determine the shift in ionic strength through the pH titration, the observed tendency in rheological parameters supports that enhancement and reduction in hydrogen bonds between gentiobiose headgroup could sensitively detected by ISR (data not shown).

**Impact of Headgroup Conformation on Viscoelastic Properties.** To further investigate the impact of conformation of carbohydrate headgroups, we measured the viscoelastic properties of Lac 1 monolayers, which has similar monosaccharide components, glycerol junction, and lipid anchors as Gent lipid. As the first step, the amplitude sweep experiments were carried out to determine the maximum strain. In contrast to that obtained for Gent monolayers (100  $\mu$ m), Lac 1 monolayers exhibited a narrower linear response regime, where the maximum strain was estimated to be 20  $\mu$ m. This indicates that Lac 1 monolayers are more viscoelastic than Gent monolayers, where the rheological response from the system already depends on the degree of deformation. Figure 5 shows  $G''$  and  $G'$  of Lac 1 and Gent monolayers as a function of area per molecule, where the corresponding pressure–area isotherms are given as insets. Note that the range of molecular area and the measurable dynamic modulus are limited due to the system. For example, the data sets of Lac 1 are determined by the onset of an increase in the isotherm (smaller than 47  $\text{\AA}^2$ ) and the measurable dynamic modulus (<30 mN/m). Nevertheless,  $G''$  and  $G'$  of Lac 1 monolayers are higher than the corresponding values of Gent monolayers under all of the measurement conditions. This can be attributed to the entropic contribution from the “bent” Gent headgroups ( $\beta$ -1 $\rightarrow$ 6 junction), which is in contrast to cylindrical Lac 1 headgroups ( $\beta$ -1 $\rightarrow$ 4 junction). In fact, the plateaulike regime (coexistence of liquid expanded and liquid condensed phases) in the pressure–area isotherm of Gent monolayer is narrower than that of Lac 1 monolayer, which coincides with

the less lateral cooperativity due to the steric effects. For comparison, the thermodynamic parameters obtained from the previous study are given in Table 1. The obtained results demonstrate the effect of carbohydrate headgroup conformation on in-plane viscoelasticity and thermodynamic phase transition.

## Conclusions

Thermodynamic phase transition and viscoelastic properties of a synthetic glycolipid with gentiobiose headgroup have quantitatively been measured using a conventional film balance technique and an interfacial stress rheometer (ISR). Strength of hydrogen bonds between headgroups are adjusted by the exchange of subphase from H<sub>2</sub>O to D<sub>2</sub>O. Although no changes could be observed between the pressure–area isotherms on two subphases, the dynamic surface moduli on D<sub>2</sub>O were almost by a factor of 2 larger than those on H<sub>2</sub>O. The obtained results thus demonstrate that ISR can detect very small changes in lateral cooperativity in carbohydrate chains at the interface. Furthermore, the comparison to a lipid with cylindrical lactose headgroup clearly revealed the entropic contribution from bent gentiobiose headgroups. Systematic combination of thermodynamics and rheology in two-dimensional glycolipid monolayers therefore enables one to study interplays of generic interactions in cell surface glycocalyx.

**Acknowledgment.** M.T. and S.S. thank E. Sackmann, M.F. Schneider, and D.A. Pink for helpful comments. This work was financially supported by National Science Foundation (NSF) through the Center on Polymer Interfaces and Macromolecular Assemblies (CPIMA), and Deutsche Forschungs Gemeinschaft (DFG Ta 259/3). M.T. is thankful to DFG for habilitation fellowship (Emmy Noether Project, Phase II).

## References and Notes

- (1) Gabius, H. J.; Gabius, S. *Glycoscience*; Chapman & Hall: Weinheim, Germany, 1997.
- (2) Curatolo, W. *Biochim. Biophys. Acta* **1987**, *906*, 137–160.
- (3) Xu, W.; Mulhern, P. J.; Blackford, B. L.; Jericho, M. H.; Firtel, M.; Beveridge, T. J. *J. Bacteriol.* **1996**, *178*, 3106–3112.
- (4) Yao, X.; Jericho, M.; Pink, D.; Beveridge, T. J. *Bacteriol.* **1999**, *181*, 6865–6875.
- (5) Brooks, C. F.; Fuller, G. G.; Franck, C. W.; Robertson, C. R. *Langmuir* **1999**, *15*, 2450–2459.
- (6) Schneider, M. F.; Lim, K.; Fuller, G. G.; Tanaka, M. *Phys. Chem. Chem. Phys.* **2002**, *4*, 1949–1952.
- (7) Schneider, M. F.; Mathe, G.; Tanaka, M.; Gege, C.; Schmidt, R. R. *J. Phys. Chem. B* **2001**, *105*, 5178–5185.
- (8) Schneider, M. F.; Zantl, R.; Gege, C.; Schmidt, R. R.; Rappolt, M.; Tanaka, M. *Biophys. J.* **2003**, *84*, 306–313.
- (9) Tanaka, M.; Schneider, M. F.; Brezesinski, G. *ChemPhysChem* **2003**, *4*, 1316.
- (10) Zhang, J.; Kovac, P. J. *Carbohydr. Chem.* **1999**, *18*, 461–469.
- (11) Abdelmageed, O. H.; Duclos Jr., R. I.; Griffin, R. G.; Siminovich, D. J.; Ruocco, M. J.; Makriyannis, A. *Chem. Phys. Lipids* **1989**, *18*, 163–169.
- (12) Gege, C.; Kinzy, W.; Schmidt, R. R. *Carbohydr. Res.* **2000**, *328*, 459–466.
- (13) Edwards, D. A.; Brenner, H.; Wasan, D. T. *Interfacial Transport Processes and Rheology*; Butterworth-Heinemann: Burlington, 1991.
- (14) Albrecht, O.; Gruler, H.; Sackmann, E. *J. Phys.* **1978**, *39*, 301–313.
- (15) *Structure and Dynamics of Membranes*; Möhwald, H., Ed.; Elsevier: Amsterdam, 1995.
- (16) Scott, H. L., Jr. *Biochim. Biophys. Acta* **1975**, *406*, 329.
- (17) Fischer, P.; Brooks, C. F.; Fuller, G. G.; Ritcey, A.; Xiao, Y.; Rahem, T. *Langmuir* **2000**, *16*, 726–734.
- (18) Dore, J. C. *J. Mol. Struct.* **1991**, *250*, 193.
- (19) Chaplin, M. F. *Biophys. Chem.* **1999**, *83*, 211.
- (20) Kjellander, R.; Florin, E. *J. Chem. Soc., Faraday Trans.* **1981**, *177*, 2053.
- (21) Naumann, C. A.; Brooks, C. F.; Fuller, G. G.; Knoll, W.; Franck, C. W. *Langmuir* **1999**, *15*, 7752–7761.